remainder or to isolate DNA of particular interest based on the initial survey make this a very practical method for examining the genomic content of environmental communities.

References and Notes

1. O. Beja *et al.*, *Science* **289**, 1902 (2000).
2. M. R. Rondon *et al.*, *Appl. Environ. Microbiol.* **66**, 2541 (2000).
3. M. H. Conte, *Oceanus* **40**, 15 (1998).
4. D. K. Steinberg *et al.*, *Deep-Sea Res. II* **48**, 1405 (2001).
5. Materials and Methods are available as supporting online material (SOM) on *Science* Online.
6. E. W. Myers *et al.*, *Science* **287**, 2196 (2000).
7. S. Karlin, C. Burge, *Trends Genet.* **11**, 283 (1995).
8. J. F. Heidelberg *et al.*, *Nature Biotechnol.* **20**, 1118 (2002).
9. For example, *Burkholderia* may be the only well-represented genus of β-Proteobacteria, with highly distinctive GC content, whereas there may be many different γ-Proteobacteria.
10. These putative strains can be easily separated post-hoc by reassembly with more stringent overlap criteria. See SOM for details.
11. G. Rocap *et al.*, *Nature* **424**, 1042 (2003).
12. B. Palenik, *Appl. Environ. Microbiol.* **60**, 3212 (1994).
13. Searches were performed on the sequences longer than 40 bp with BLASTx against the entire nraa data set archived at GenBank.
14. B. Boeckmann *et al.*, *Nucleic Acids Res.* **31**, 365 (2003).
15. M. J. Chretiennotdinet *et al.*, *Phycologia* **34**, 285 (1995).
16. L. Guillou *et al.*, *J. Phycol.* **35**, 368 (1999).
17. J. R. Cole *et al.*, *Nucleic Acids Res.* **31**, 442 (2003).
18. C. A. Carlson *et al.*, *Aquat. Microb. Ecol.* **30**, 19 (2002).
19. J. A. Klappenbach, J. M. Dunbar, T. M. Schmidt, *Appl. Environ. Microbiol.* **66**, 1328 (2000).
20. A. Chao, *Scand. J. Stat.* **11**, 265 (1984).
21. T. P. Curtis, W. T. Sloan, J. W. Scannell, *Proc. Natl. Acad. Sci. U.S.A.* **99**, 10494 (2002).
22. S. Giovanonni, M. S. Rappe, in *Microbial Ecology of the Oceans*, D. L. Kirchman, Ed. (Wiley, New York, 2000), pp. 47–84.
23. M. S. Rappe, S. A. Connon, K. L. Vergin, S. J. Giovannoni, *Nature* **418**, 630 (2002).
24. J. Raymont, *Plankton and Productivity in the Oceans* (William Clowes Limited, London, ed. 2, 1980).
25. T. Parsons, M. Takahashi, B. Hargrave, *Biological Oceanographic Processes* (BPCC Wheatons Ltd., Exeter, UK, ed. 3, 1984).
26. J. E. Hobbie, R. J. Daley, S. Jasper, *Appl. Environ. Microbiol.* **33**, 1225 (1977).
27. P. del Giorgio, Y. Prairie, D. Bird, *Microb. Ecol.* **34**, 144 (1997).
28. A. Alldredge, Y. Cohen, *Science* **235**, 689 (1987).
29. E. F. DeLong, D. Franks, A. Alldredge, *Limnol. Oceanogr.* **38**, 924 (1993).
30. U. Passow, *Prog. Oceanogr.* **55**, 287 (2002).
31. K. H. Nealson, J. Scott, in *The Prokaryotes: An Evolving Electronic Resource for the Microbiological Community*, E. A. Dworkin, Ed. (Springer-Verlag, NY, 2003).
32. C. L. Hicks, R. Kinoshita, P. W. Ladds, *Aust. Vet. J.* **78**, 193 (2000).
33. The criteria for this filtering were that more than 50% of the assembly had a database hit and more than 30% of the sequence had the best hit to archaeal gene sequences.
34. J. L. Stein, T. L. Marsh, K. Y. Wu, H. Shizuya, E. F. DeLong, *J. Bacteriol.* **178**, 591 (1996).
35. M. Breitbart *et al.*, *Proc. Natl. Acad. Sci. U.S.A.* **99**, 14250 (2002).
36. L. M. Proctor, J. A. Fuhrman, *Nature* **343**, 60 (1990).
37. K. K. Cavender-Bares, D. M. Karl, S. W. Chisholm, *Deep-Sea Res. I* **48**, 2373 (2001).
38. O. Beja *et al.*, *Science* **289**, 1902 (2000).
39. J. R. de la Torre *et al.*, *Proc. Natl. Acad. Sci. U.S.A.* **100**, 12830 (2003).
40. O. Beja, E. N. Spudich, J. L. Spudich, M. Leclerc, E. F. DeLong, *Nature* **411**, 786 (2001).
41. G. Sabehi *et al.*, *Environ. Microbiol.* **5**, 842 (2003).
42. M. Guerero, R. Jones, *Mar. Ecol. Prog. Ser.* **141**, 193 (1996).
43. M. Guerrero, R. Jones, *Mar. Ecol. Prog. Ser.* **141**, 183 (1996).
44. B. Palenik *et al.*, *Nature* **424**, 1037 (2003).
45. D. Scanlan *et al.*, *Appl. Environ. Microbiol.* **63**, 2411 (1997).
46. D. Scanlan, W. H. Wilson, *Hydrobiologia* **401**, 149 (1999).

47. The authors would like to acknowledge P. Lethaby, M. Roadman, D. Clougherty, N. Buck, J. Selengut, A. Delcher, M. Pop, H. Koo, R. Doering, M. Wu, J. Badger, K. Moffat, S. Yooseph, E. Kirkness, D. Karl, K. Heidelberg, B. Friedman, H. Kowalski, and the staff of the J. Craig Venter Science Foundation Joint Technology Center. We also acknowledge the help of N. Nelson at UCSB-ICESS for assistance in acquiring the satellite image in Fig. 1. Further, we acknowledge the NSF Division of Ocean Sciences for its ongoing support of the BATS Program and the RV Weatherbird II, and the Department of Energy Genomes to Life program for its support of K. Nealson. This research was supported by the Office of Science (B.E.R.), U.S. Department of Energy grant no. DE-FG02-02ER63453, and the J. Craig Venter Science Foundation. This is contribution No. 1646 of the Bermuda Biological Station for Research, Inc.

Supporting Online Material

www.sciencemag.org/cgi/content/full/1093857/DC1
Materials and Methods
SOM Text
Figs. S1 to S10
Tables S1 to S5
References

20 November 2003; accepted 20 February 2004
Published online 4 March 2004;
10.1126/science.1093857
Include this information when citing this paper.

REPORTS

Approaching the Quantum Limit of a Nanomechanical Resonator

M. D. LaHaye,[1,2] O. Buu,[1,2] B. Camarota,[1,2] K. C. Schwab[1]*

By coupling a single-electron transistor to a high–quality factor, 19.7-megahertz nanomechanical resonator, we demonstrate position detection approaching that set by the Heisenberg uncertainty principle limit. At millikelvin temperatures, position resolution a factor of 4.3 above the quantum limit is achieved and demonstrates the near-ideal performance of the single-electron transistor as a linear amplifier. We have observed the resonator's thermal motion at temperatures as low as 56 millikelvin, with quantum occupation factors of N_{TH} = 58. The implications of this experiment reach from the ultimate limits of force microscopy to qubit readout for quantum information devices.

Since the development of quantum mechanics, it has been appreciated that there is a fundamental limit to the precision of repeated position measurements (*1*). This is a consequence of the Heisenberg uncertainty principle (*2*), which places a limit on the simultaneous knowledge of position x and momentum p: $\Delta x \cdot \Delta p \geq \frac{\hbar}{2}$, where $2\pi \cdot \hbar$ is Planck's constant. When applied to a simple harmonic oscillator of mass m and angular resonant frequency ω_0, this relationship places a limit on the precision of two instantaneous, strong position measurements, what is called the "standard quantum limit," $\Delta x_{SQL} = \sqrt{\frac{\hbar}{2m\omega_0}}$ (*3*).

Although the standard quantum limit captures the physics of the uncertainty principle, it is far from the situation found when one continuously measures the position with a linear detector. Linear amplifiers not only detect and amplify the incoming desired signal but also impose back-action onto the object under study (*4*); the current noise emanating from the input of a voltage preamplifier or the momentum noise imparted to a mirror in an optical interferometer are manifestations of this back-action. The uncertainty principle again appears and places a quantum limit on the minimum possible back-action for a linear amplifier. Previous work (*5*) has concluded that the minimum possible amplifier noise temperature is $T_{QL} = \frac{\hbar\omega_0}{\ln 3 \cdot k_B}$. Applying this result to the continuous readout of a simple harmonic oscillator yields the ultimate position resolution (*6*): $\Delta x_{QL} = \sqrt{\frac{\hbar}{\ln 3 \cdot m\omega_0}} \approx 1.35 \cdot \Delta x_{SQL}$, which

[1]Laboratory for Physical Sciences, 8050 Greenmead Drive, College Park, MD 20740, USA. [2]Department of Physics, University of Maryland, College Park, MD 20740, USA.

*To whom correspondence should be addressed. E-mail: schwab@lps.umd.edu

accounts for both the quantum noise of the resonator and the linear amplifier.

In addition to issues of ultimate limits of measurement, it has been recently appreciated (*7*) that it should be possible to prepare micron-scale, resonant mechanical systems in the quantum ground state. The energy of this elementary system should be quantized: $E_N = \hbar\omega_0(N + 1/2)$, where $N = 0,1,2, \ldots$, with a minimum possible energy of $E_0 = \hbar\omega_0/2$ corresponding to an average position $\bar{x} = 0$ and standard deviation of Δx_{SQL}. Freeze-out to the quantum ground state should occur when $k_B T/\hbar\omega_0 = T/T_Q \leq 1$. As a result of the high resonance frequency of nanomechanics, now demonstrated as high as 1 GHz (*8*), freeze-out should be possible at millikelvin temperatures. We demonstrate the approach to the quantum limit of a 19.7-MHz nanomechanical resonator in both of these ways: continuous position observation approaching the uncertainty principle limit and observation of low quantum numbers by thermalization to millikelvin temperatures.

To approach these limits, we have engineered a nanoelectromechanical system composed of a microscopic mechanical resonator capacitively coupled to a superconducting single-electron transistor (SSET) (Fig. 1). The mechanical resonator is biased with a large dc potential, V_{NR}, and coupled to the SSET island through C_G. In-plane motion of the resonator linearly modulates this capacitance and thus changes the potential of the island, which, in turn, changes the impedance of the SSET. Use of a microwave matching network [radio frequency SSET (RF-SSET)] technique (*4*) allows continuous readout of the SSET impedance with very high sensitivity and bandwidth (*9*) (fig. S1). This position-detection scheme and potential for approaching quantum limits has been considered by a number of authors (*10*–*12*) and has very recently been demonstrated (*13*) with a normal-state single-electron transistor (SET), albeit with very limited bandwidth and sensitivity far from the quantum limit.

A SSET is thought to be a realization of a near-ideal linear amplifier, ideal in the sense that amplification can be accomplished with back-action close to that which is required by the uncertainty principle (*4*, *14*). The back-action is a result of the electrons stochastically tunneling onto and off of the island, changing its potential by $\delta V = \frac{e}{C_\Sigma} \sim 400\ \mu V$ with each tunneling event, where $C_\Sigma \sim 400$ aF is a typical total island capacitance. Calculations of the spectral power density of these fluctuations for an SSET show a white power spectrum extending up to $1/R_\Sigma C_\Sigma \sim 10$ GHz, with an amplitude of $\sqrt{S_V} = \sqrt{\frac{e^3}{I_{DS} C_\Sigma^2}} \sim 3nV/\sqrt{Hz}$ (*14*, *15*). These voltage fluctuations produce back-action forces and stochastic displacements of the mechanical resonator, ultimately limiting the position resolution of this scheme. Thus, careful attention must be placed upon the engineering of the coupling between the mechanical resonator and the SSET (*10*, *11*). As the coupling voltage, V_{NR}, is increased, the SSET becomes more sensitive to displacements, with the resolution limited by the shot-noise through the SSET. However, as V_{NR} is increased, coupling to the back-action voltage fluctuations of the island becomes stronger, ultimately overcoming the increase in position sensitivity. Fig. 1 shows the predicted sensitivity versus coupling voltage V_{NR} (*10*, *11*) using our demonstrated device parameters. Optimal detection approaches the quantum limit at $V_{NR} \sim 13$ V, although given the nonideality of our RF-SSET readout, we do not expect to be limited by back-action until $V_{NR} \sim 27$ V.

Figure 2 shows the sample layout and the details of the RF-SSET coupled to the nanomechanical resonator. An on-chip LC resonator is microfabricated for impedance matching the SSET to an ultralow noise, 50 Ω microwave amplifier with $T_N = 2$ K. The LC resonator is formed by an interdigitated capacitor and a planar Al coil (14 turns, 130 μm square, 1 μm pitch and line width). Our circuit demonstrates a resonance at 1.35 GHz with a $Q \sim 10$, giving a detection bandwidth of ~70 MHz. The SSET characteristics measured through the mapping of I_{DS} versus V_{DS} versus V_{NR} are $C_\Sigma = 450$ aF, $C_G = 26$ aF, and $R_\Sigma = 70$ kΩ where R_Σ is the series resistance of the tunnel junctions; we achieve a charge sensitivity of $\sqrt{S_Q} \cong 6 - 14\ \mu e/\sqrt{Hz}$. A feedback scheme is used to sense and hold the SSET at maximum charge sensitivity (*9*). This is essential for achieving the best position sensitivity, because the noise floor of our RF-SSET is determined by the cryogenic microwave preamplifier. We achieve gain stability sufficient for long-term averages of the noise spectra.

The nanomechanical resonances of the doubly clamped beam are first identified using magnetomotive readout (*16*); we find an out-of-plane resonance of 17 MHz and an in-plane resonance of 19.7 MHz. Fig. 3 shows the in-plane mode detected with the RF-SSET. The two displacement detection techniques give identical resonator characteristics within measurement uncertainty. From the temperature dependence of the quality factor of the 19.7-MHz mode (Fig. 4), it is interesting to note the linear increase in quality factor as temperature decreases, a much stronger dependence than what is uniformly observed in nanomechanical resonators at higher temperatures (*17*).

Without driving the resonance and simply recording the noise spectra from the RF-SSET, we can detect the thermal motion of the beam at very low temperatures (Fig. 3). The noise power fits a simple harmonic oscillator line shape, sitting atop a white-noise background from the cryogenic preamplifier, with frequency and Q identical to that found by driving.

The integrated noise power is proportional to $\langle x^2 \rangle$ and is plotted versus temperature (Fig. 4). Above 100 mK, it closely follows a linear temperature dependence with intercept through the origin. As our mechanical mode is essentially classical for temperatures above $T_Q = \frac{\hbar\omega_0}{k_B} =$ 1 mK, this is the expected result, which follows from the classical equipartition of energy: $\langle E \rangle = m\omega_0^2\langle x^2 \rangle = k_B T$. Analogous to Johnson noise thermometry (*18*), this technique allows direct measurement of the thermodynamic temperature of the nanomechanical mode (*9*).

Below 100 mK, we observe that the integrated noise power does not follow the same linear dependence as we continue to cool the sample holder to 35 mK (temperature measured by RuO-resistance thermometry mounted on the Cu sample package.) A possible reason for this excess mechanical noise temperature is

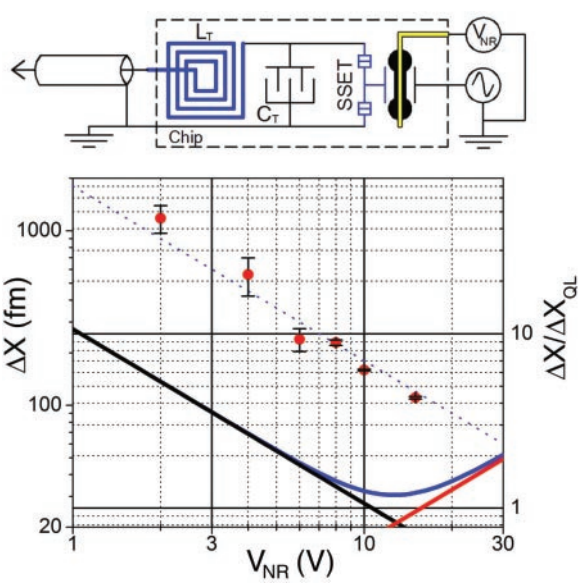

Fig. 1. (**Bottom**) The solid lines show the expected position resolution due to shot-noise (black), back-action noise (red), and the uncorrelated sum (blue) as a function of coupling voltage V_{NR}, assuming the device parameters realized in this experiment. The points are the observed sensitivity where the deviation from the blue curve is due to nonidealities in the RF-SSET readout circuit. The dashed line is the expected sensitivity calculated from the measured charge sensitivity. Error bars are on the quantity $\Delta X/\Delta X_{QL}$. (**Top**) The simplified schematic shows the RF-SSET capacitively coupled to a voltage-biased Au/SiN nanomechanical resonator with on-chip LC resonator formed by the square spiral, L_T, and an interdigitated capacitor, C_T.

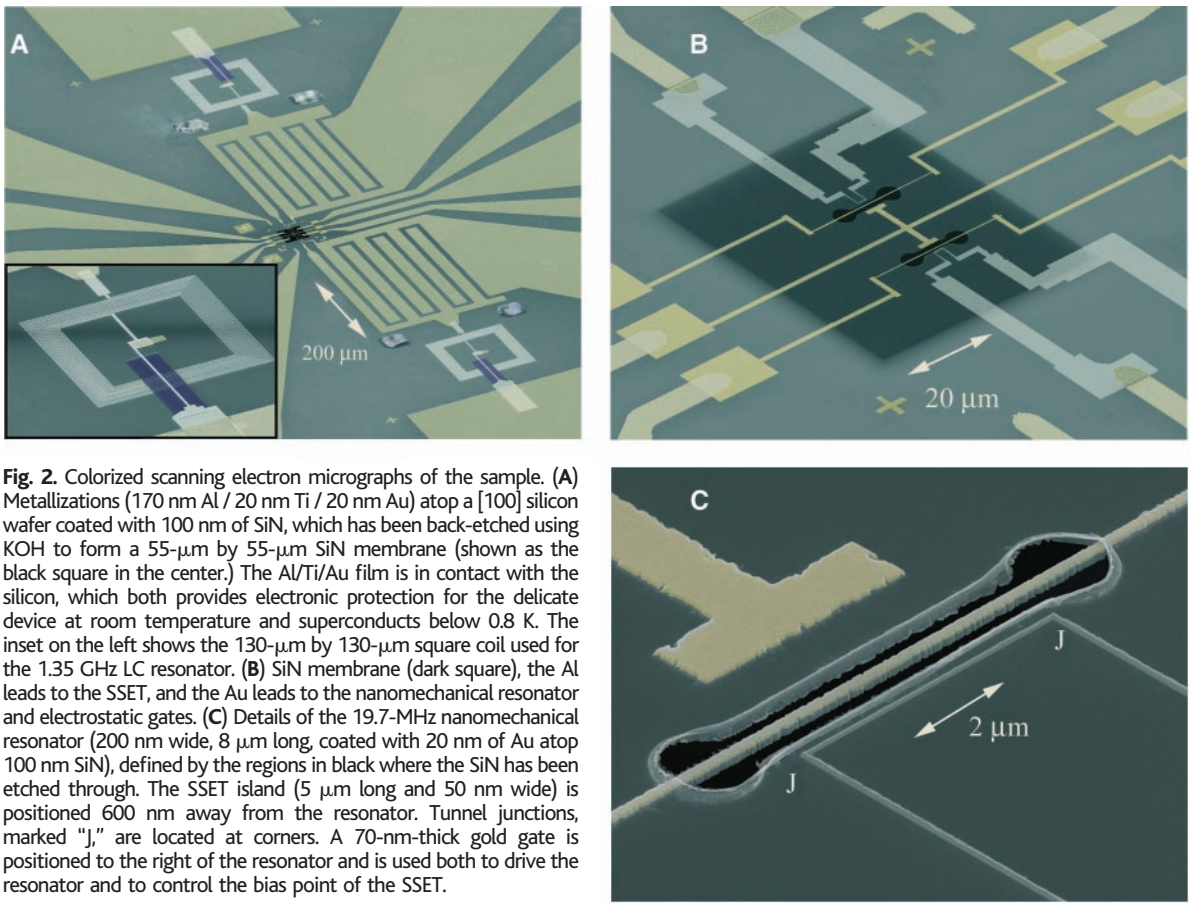

Fig. 2. Colorized scanning electron micrographs of the sample. (**A**) Metallizations (170 nm Al / 20 nm Ti / 20 nm Au) atop a [100] silicon wafer coated with 100 nm of SiN, which has been back-etched using KOH to form a 55-μm by 55-μm SiN membrane (shown as the black square in the center.) The Al/Ti/Au film is in contact with the silicon, which both provides electronic protection for the delicate device at room temperature and superconducts below 0.8 K. The inset on the left shows the 130-μm by 130-μm square coil used for the 1.35 GHz LC resonator. (**B**) SiN membrane (dark square), the Al leads to the SSET, and the Au leads to the nanomechanical resonator and electrostatic gates. (**C**) Details of the 19.7-MHz nanomechanical resonator (200 nm wide, 8 μm long, coated with 20 nm of Au atop 100 nm SiN), defined by the regions in black where the SiN has been etched through. The SSET island (5 μm long and 50 nm wide) is positioned 600 nm away from the resonator. Tunnel junctions, marked "J," are located at corners. A 70-nm-thick gold gate is positioned to the right of the resonator and is used both to drive the resonator and to control the bias point of the SSET.

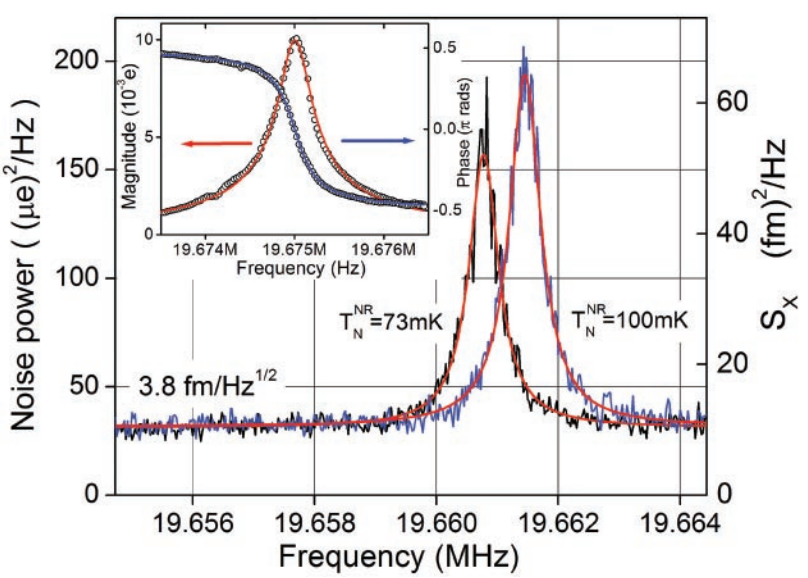

Fig. 3. Charge noise power around the mechanical resonance with V_{NR} = 15 V. Right peak is taken at 100 mK and is fit with a Lorentzian, shown as a red line. This noise power is used to scale the left peak taken with the refrigerator at 35 mK and corresponds to a resonator noise temperature of T_N^{NR} = 73 mK. This then scales the white-noise floor, which corresponds to a system-noise temperature of T_N^{SSET} = 16 mK = 18 T_{QL}. Using the equipartition relation, the displacement resolution is 3.8 fm/$\sqrt{\text{Hz}}$. The inset shows the driven response, approximately 800 pm on resonance, with the data as circles and a Lorentzian fit as the solid lines. All SSET measurements are taken with the SSET biased near the double Josephson quasiparticle resonance peak.

through electrostatic fluctuations from the SSET back-action or on nearby gates. This does not appear to be the case, because the behavior is independent of coupling voltage, as shown in Fig. 4. Excess noise temperatures due to electrostatic fluctuations from any source should produce a quadratic dependence with V_{NR}, which is clearly not observed (*12*, *19*). We also rule out a long thermal relaxation time, because the refrigerator is run continuously at base temperature for 72 hours and we see no sign of continued cooling. Nonetheless, we observe a mechanical mode with noise temperature of T_N^{NR} = 56 mK, and a corresponding quantum occupation factor of N = T_N^{NR}/T_Q = 58.

The most likely cause of the excess noise temperature below 100 mK is the ~2 pW dissipated in the SSET, which locally heats the SiN membrane around the nanomechanical resonator. A simple thermal model using the measured thermal conductance of a SiN membrane (*20*) shows that the dissipated power is expected to increase the local temperature around the resonator by ~50 mK. This might be remedied by placing the SSET on the Si substrate and coupling to the nanomechanical resonator through a coupling capacitor. This would allow the hot phonons

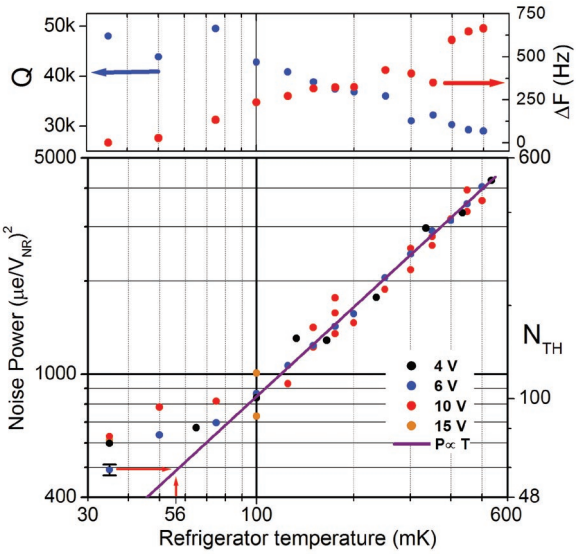

Fig. 4. The integrated charge noise power, PNR, scaled by V_{NR}, versus refrigerator temperature for different V_{NR}. Right axis shows the quantum occupation factor, N_{TH}. Above 100 mK, we find excellent agreement with classical equipartition of energy, $P_{NR} \propto T$, shown as the solid line through the origin. Below 100 mK, we observe a deviation from this relationship, indicating a difficulty in thermalizing the nanomechanical mode. The arrow indicates the lowest observed noise temperature, $T_N^{NR} = 56$ mK and $N_{TH} = 58$. The upper plot shows both the quality factor, Q, and the resonant frequency shift, $\Delta F = F(T) - F(35\ mK)$, versus temperature, which are extracted by fitting the thermal noise peaks at $V_{NR} = 6$ V.

emitted by the SSET to radiate away ballistically into the substrate.

For our highest couplings, we do observe substantial scatter in the mechanical noise temperature, beyond the statistical uncertainty (Fig. 4). Changes in mechanical noise temperature are accompanied by sudden changes in resonator frequency of 100 to 300 Hz, changes in resonator quality factor of 10%, and changes in RF-SSET sensitivity of 30%. This behavior was not observed in a nearly identical sample that showed much higher stability for large V_{NR} but was unfortunately destroyed before a complete study could be made.

Because we observe no clear evidence of back-action, the noise temperature of our SSET measurement scheme can be evaluated from the spectrum shown in Fig. 3. With $V_{NR} = 15$ V, we find that the noise temperature of our displacement-sensing scheme at the mechanical resonance is $T_N^{SSET} = 16\ mK = 17\ \hbar\omega_0 = 18\ T_{QL}$, which gives a position standard deviation of $\Delta x = \sqrt{\frac{T_N^{SSET}}{T_{QL}}} \cdot \Delta x_{QL} = 4.3 \cdot \Delta x_{QL}$. The position sensitivity of our detection scheme can be estimated with the equipartition relationship and our estimate of the resonator mass, $m_{eff} = 9.7 \cdot 10^{-16}$ kg (*21*). Our best position sensitivity is $\sqrt{S_x} = 3.8\ fm/\sqrt{Hz}$. At base temperature, we find a quality factor of $Q = 3.5 \cdot 10^4$, which gives an effective noise bandwidth of $\Delta f = \omega_0/4Q = 903$Hz and a position standard deviation of $\Delta x = 114\ fm$ with $\Delta x_{QL} = 26\ fm$. This is the closest approach to the uncertainty principle limit on position measurement to date. Further optimization of the SSET charge readout by improving our microwave amplifier would allow a closer approach to the minimum shown in Fig. 1, with $\Delta x \approx 1.5 \cdot \Delta x_{QL}$ appearing technically possible (*4*).

Although our measurements at 20 MHz are essentially immune to nonintrinsic noise, which is ubiquitous at acoustic frequencies, it is interesting to compare our approach to the quantum limit with the current sensitivity of ultrasensitive gravitational wave detectors. The 4-km Laser Interferometer Gravitational-Wave Observatory (LIGO) interferometric detector has achieved $\Delta x = 1000 \cdot \Delta x_{QL}$ (*22*) at 100 Hz. A tabletop optical interferometer has achieved $\Delta x = 23 \cdot \Delta x_{QL}$ on the 2 MHz vibrational modes of a 100-g silica mirror at room temperature (*23*). The best performance on the readout of displacement transducers for cryogenic, acoustic gravitational wave detectors at 1 KHz is $\Delta x = 167 \cdot \Delta x_{QL}$ (*24*), with thermal occupation $N_{TH} \sim 10^9$.

The recent demonstration of nanomechanical displacement detection with an SET mixer (*13*) achieved similar position sensitivity $\sqrt{S_x}$ on a 100-MHz resonator, but because of the much lower quality factor, larger noise equivalent bandwidth, and lower quantum limit of motion, the standard deviation of position achieved was far from the quantum limit: $\Delta x = 100 \cdot \Delta x_{QL}$. This detection scheme did not possess sufficient bandwidth or sensitivity to observe the mechanical mode temperature.

The level of position sensitivity and the approach to low quantum numbers demonstrated here open the possibility for a wealth of nanoelectromechanics experiments at millikelvin temperatures: observation of mesoscopic fluctuations in nanomechanics (*25*), quantum-limited feedback cooling (*26*), and quantum squeezing (*3*). By improving the thermal characteristics of our sample and increasing the frequency of the mechanical mode, we expect to approach freeze-out to the quantum ground state, which should show deviations from the classical equipartition of energy and evidence for energy quantization and zero-point motion. In addition, there has been theoretical work suggesting the possibility of observing coherent quantum behavior of a nanomechanical device interacting with a superconducting two-level system (a Cooper-Pair box) (*27*, *28*). Two critical parameters in this scheme are the mode temperature, which should determine the coherence time, and the interaction strength, which is a function of $C_G V_{NR}$. Using the parameters demonstrated in this work (Q, T_N^{NR}, $C_G V_{NR}$), we expect the interaction to approach the strong coupling limit $\langle H_I \rangle \sim \hbar\omega_0$ and the mechanical coherence time to be long enough ($\sim$1 μsec), allowing the possible formation of entangled states and ultimately tests of quantum mechanics at the micron scale and beyond (*29*).

References and Notes

1. L. D. Landau, R. Peierls, *Z. Phys.* **69**, 56 (1931).
2. W. Heisenberg, *Z. Phys.* **43**, 172 (1927).
3. V. B. Braginsky, F. Ya. Khalili, *Quantum Measurement* (Cambridge Univ. Press, Cambridge, 1995), pp. 12–15.
4. M. H. Devoret, R. J. Schoelkopf, *Nature* **406**, 1039 (2000).
5. C. M. Caves, *Phys. Rev. D* **26**, 1817 (1982).
6. C. M. Caves, K. S. Thorne, W. P. Drever, V. D. Sandberg, N. Zimmermann, *Rev. Mod. Phys.* **52**, 341 (1980).
7. M. L. Roukes, *Phys. World* **14**, 25 (2001).
8. X. Ming, H. Huang, C. A. Zorman, M. Mehregany, M. L. Roukes, *Nature* **421**, 496 (2003).
9. Materials and methods are available as supporting material on *Science* Online.
10. M. P. Blencowe, M. N. Wybourne, *Appl. Phys. Lett.* **77**, 3845 (2000).
11. Y. Zhang, M. P. Blencowe, *J. Appl. Phys.* **91**, 4249 (2002).
12. D. Mozyrsky, I. Martin, *Phys. Rev. Lett.* **89**, 018301 (2002).
13. R. G. Knobel, A. N. Cleland, *Nature* **424**, 291 (2003).
14. A. A. Clerk, S. M. Girvin, A. K. Nguyen, A. D. Stone, *Phys. Rev. Lett.* **89**, 176804 (2002).
15. A. N. Korotkov, *Phys. Rev. B* **49**, 10381 (1994).
16. D. S. Greywall, B. Yurke, P. A. Busch, A. N. Pargellis, R. L. Willett, *Phys. Rev. Lett.* **72**, 2992 (1994).
17. A. B. Hutchinson *et al.*, *Appl. Phys. Lett.* **84**, 972 (2004).
18. F. Pobell, *Matter and Methods at Low Temperatures* (Springer-Verlag, New York, ed. 2, 1996).
19. A. D. Armour, M. P. Blencowe, Y. Zhang, *Phys. Rev. B* **69**, 125313 (2004).
20. M. M. Leivo, J. P. Pekola, *Appl. Phys. Lett.* **72**, 1305 (1998).
21. The effective mass of the resonator is calculated by assuming that the stored energy is that of a doubly clamped beam with stiffness as the restoring force, and integrating the average displacement over the 5-μm overlap between the SSET island and the resonator. We find that $m_{eff} = 0.686 \cdot m$, where m is the mass of the entire resonator.
22. B. Abbott *et al.*, http://arxiv.org/abs/gr-qc/0308069 (2003).
23. Y. Hadjar *et al.*, *Europhys. Lett.* **47**, 545 (1999).
24. G. M. Harry, Insik Jin, Ho Jung Paik, T. R. Stevenson, F. C. Wellstood, *Appl. Phys. Lett.* **76**, 1446 (2000).
25. A. V. Shytov, L. S. Levitov, C. W. J. Beenakker, *Phys. Rev. Lett.* **88**, 228303 (2002).
26. A. Hopkins, K. Jacobs, S. Habib, K. Schwab, *Phys. Rev. B* **68**, 235328 (2003).
27. A. D. Armour, M. P. Blencowe, K. C. Schwab, *Phys. Rev. Lett.* **88**, 148301 (2002).
28. E. K. Irish, K. Schwab, *Phys. Rev. B* **68**, 155311 (2003).
29. A. J. Leggett, *J. Phys. Cond. Matter* **14** R415 (2002).

30. We would like to acknowledge very helpful conversations with C. Sanchez, M. Blencowe, A. Armour, M. Roukes, K. Jacobs, S. Habib, A. Korotkov, A. Buonanno, and K. Ekinci. This work has been supported by the U.S. Department of Defense.

Supporting Online Material

www.sciencemag.org/cgi/content/full/304/5667/74/DC1
Materials and Methods
Fig. S1

8 December 2003; accepted 12 February 2004